THE ROLE OF COAGULATION AND SEDIMENTATION MECHANISMS IN THE TWO-COMPONENT MODEL OF SEA-PARTICLE SIZE DISTRIBUTION

DUBRAVKO RISOVIĆ and MLADEN MARTINIS

Rugjer Bošković Institute, P.O.B. 1016, 41001 Zagreb, Republic of Croatia

Simple coagulation and sedimentation mechanisms are considered in relation to the sea particle size distribution (PSD). It is shown that the values of γ-parameters in the two-component model of PSD can be associated with coagulation and sedimentation mechanisms. Moreover, it is shown that low γ_A-values can be associated with high turbulent kinetic energy dissipation rate characteristic of surface and coastal waters. High γ_A-values, characteristic of deep waters, indicate domination of differential sedimentation over shear coagulation. An insight into the size ordering of mechanisms and the extent of size sub-range in which they dominate can be inferred from generalized power exponent $m(r)$ which is γ-parameter dependent.

1. Introduction

It has been shown that the shape of a sea particle size distribution (PSD) can be (at least partially) attributed to the simple coagulation and sedimentation mechanisms [1-4]. Attempts to find the connection between the shape of the marine-particle size distribution and various mechanisms are not new, and yet the problem is not fully resolved. One point of interest is to find the mechanisms which are

responsible for the particle size distribution, starting from the properties of the functions which best fit the experimental data.

Various mechanisms influencing PSD have been considered, including dissolution [5,6], sedimentation of individual particles [1,3,8] and fecal pellets [8]. More recent investigations have confirmed the crucial role of aggregation and sedimentation mechanisms in transport, dynamics and size distribution of sea particles [9-13].

The aim of this paper is to establish the connection between recently introduced two-component model (TCM) of PSD [15] and predictions obtained from consideration of basic physical mechanisms, namely coagulation and sedimentation. In particular, to show that the values of the γ-parameters in the TCM are mechanism-dependent, and therefore could be used to infer information regarding dominant mechanisms underlying particular PSD.

2. Coagulation and sedimentation mechanisms and PSD

In natural and polluted waters there exists a continuous distribution of particle sizes most appropriately described by:

$$\mathrm{d}N = n(r)\mathrm{d}r \tag{1}$$

where $\mathrm{d}N$ is a number of particles per unit fluid volume with radii between r and $r + \mathrm{d}r$.

Considering the PSD, we shall assume that the changes are due to coagulation and sedimentation only. Sedimentation is a mechanism by which particles are removed from considered volume, and coagulation transfers particles from one part of the distributions to another part, as many smaller particles form few larger particles.

Coagulation and sedimentation, in relation to PSD, were studied by many authors [1,2,4,16,17], and we shall start by rewieving some of the results.

2.1. Coagulation

The rate at which particles are lost from sizes r_i and r_j due to coagulation is

$$\beta_{ij}(r_i, r_j)n(r_i)\mathrm{d}r_i n(r_j)\mathrm{d}r_j \tag{2}$$

where $\beta_{ij}(r_i, r_j)$ is the collision function determined by the particular coagulation mechanism,

$$\beta_{ij}(r_i, r_j) = E_{ij}K_{ij}(r_i, r_j).$$

K_{ij} is mechanism-dependent, second order rate coefficient that describes the frequency at which particles are brought into close proximity, and E_{ij} is the probability that two particles do make contact once they are in close proximity ("contact efficiency").

There are three coagulation mechanisms, each with a different collision function.

Coagulation of smallest particles is governed primarily by thermal (Brownian) motion, and the collision rate coefficient for spherical particles neglecting van der Waals and other forces has been found [18,19] to be given by:

$$K_b(r_i, r_j) = \frac{2}{3} \frac{kT}{\mu} \frac{(r_i + r_j)^2}{r_i r_j} \tag{3}$$

where k is the Boltzmann constant, μ is the dynamic fluid viscosity and T absolute temperature.

In a laminary or turbulent flow, there is a fluid shear causing particles to collide. The collision rate coefficient for particles smaller than the Kolmogorov scale is proportional to the mean shear rate G, and given by [20,21]:

$$K_{sh}(r_i, r_j) = \frac{4}{3} G(r_i + r_j)^3. \tag{4}$$

For a laminar flow the mean shear rate G is given by velocity gradient, and for a turbulent flow it is approximated by $G = (\varepsilon/\nu)^{1/2}$, where ε is the rate of turbulent energy dissipation, and ν the kinematic viscosity of the fluid [17].

Coagulation due to different particle settling velocities (differential sedimentation) has the collision rate coefficient depending on difference in Stoke's settling velocities among particles i and j,

$$K_{ds}(r_i, r_j) = \frac{2\pi g}{9\nu} \left(\frac{\rho_p - \rho_f}{\rho_f} \right) (r_i + r_j)^2 |r_i^2 - r_j^2| \tag{5}$$

where g is gravitational acceleration and ρ_p and ρ_f are particle and fluid densities, respectively.

2.2. Sedimentation

Stoke's law for the settling flux F of particles with sizes between r_i and $r_i + \mathrm{d}r_i$ is given by:

$$F = \frac{2\pi g}{9\nu} \left(\frac{\rho_p - \rho_f}{\rho_f} \right) r_i^2 n(r_i) \mathrm{d}r_i \tag{6}$$

where ρ_f and ρ_p are the respective densities of fluid and particle.

Solution of a general equation for PSD, including all mechanisms, is very difficult. However, useful solutions can be found if one assumes that only one coagulation or sedimentation mechanism is dominant in a given sub-range of particle sizes. These sub-ranges can be found by comparison of collision functions associated with each mechanism. According to Hunt [2], the order of dominant mechanisms, with increasing size of colliding particles (starting from very small particles) is: Brownian coagulation, shear coagulation and coagulation due to the differential sedimentation, while for very large particles the dominant particle removal mechanism is gravitational settling. If one assumes that the PSD is in a dynamic steady state, and using the dimensional analysis, one can derive the PSD resulting from each mechanism. For regions dominated by Brownian, shear, differential sedimentation and settling the predicted size distributions are [2,17]:

a) Brownian coagulation:

$$n(r) = A_B \left(\frac{E}{B} \right)^{1/2} r^{-2.5}, \qquad (7)$$

where A_B is a dimensionless constant, $B = kT/\mu$ and E the flux of particle volume.

b) Shear coagulation:

$$n(r) = A_{sh} \left(\frac{E}{G} \right)^{1/2} r^{-4}. \qquad (8)$$

c) Differential sedimentation:

$$n(r) = A_{ds} \left(\frac{E}{D} \right)^{1/2} r^{-4.5} \qquad (9)$$

where $D = g(\rho_p - \rho_f)/\rho_f \nu$ and A_{ds} is a dimensionless constant.

d) Settling:

$$n(r) = A_s \left(\frac{E}{S} \right)^{3/4} r^{-4.75} \qquad (10)$$

where $S = (g/\nu)(\rho_p - \rho_f)/\rho_f$ and A is a dimensionless constant.
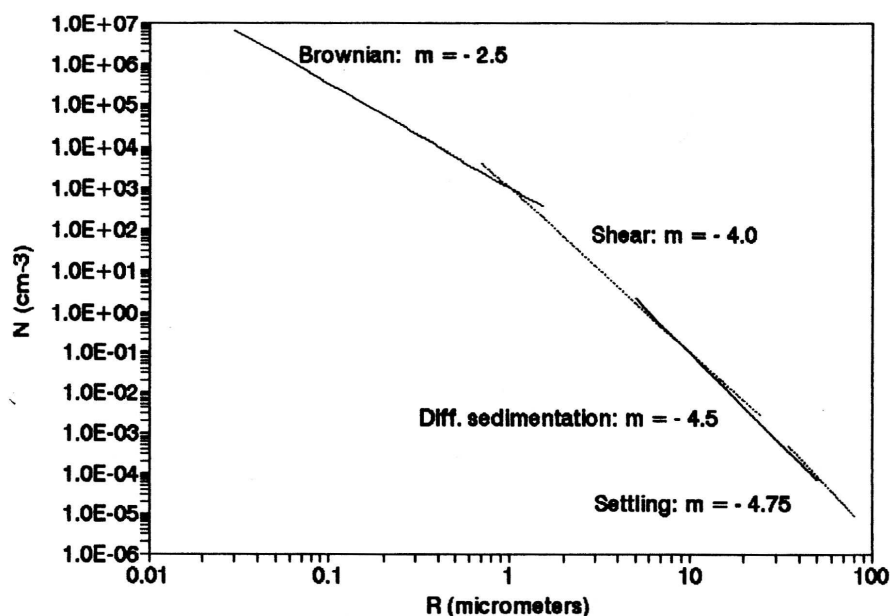
Fig. 1. Hypothetical particle size distribution resulting from various mechanisms. Each mechanism generates a different slope of PSD. Mechanism/size-range order and extent of overlap regions is obtained from comparison of mechanism collision frequencies in a certain sub-range. Assumption of unit contact efficiency leads to depicted order, while inclusion of size dependent contact efficiency leads to a mechanism/size-range order which depends on turbulent energy dissipation rate.

When plotted on log-log scales, these distributions are represented by straight lines with slopes −2.5, −4, −4.5 and −4.75, respectively, resulting in segmented power distribution shown in Fig. 1. It could represent the real situation if only one mechanism is dominant in a given particle sub-range. However, there is no clear border between these single-mechanism dominated sub-ranges. Rather, there are overlap regions where two mechanisms are simultaneously responsible for the formation of PSD. These regions are shown in Fig. 1 by a schematic overlap of power-law segments. The width of these overlap regions may vary considerably, depending on physical situation. Furthermore, one may expect that in these regions exponent in the power-law approximating PSD will be different from the above cited exponents. Unfortunately, this problem can not be solved by similarity methods or dimensional analysis.

To examine this more closely, we first turn briefly to the recently introduced two-component model (TCM) of PSD [15] and establish the relation to coagulation and sedimentation mechanisms.

3. Coagulation and sedimentation in connection with TCM

The TCM predicts PSD as a superposition of two components A and B:

$$\mathrm{d}N(r) = n_A(r)\mathrm{d}r + n_B(r)\mathrm{d}r = C_A F_A(r)\mathrm{d}r + C_B F_B(r)\mathrm{d}r \tag{11}$$

$$F_A(r) = r^2 e^{-52r^{\gamma_A}} \tag{12}$$

$$F_B(r) = r^2 e^{-17r^{\gamma_B}} \tag{13}$$

where γ_A and γ_B are parameters of the distribution, and C_A and C_B are constants related to the concentration of the respective components. To avoid dimensional problems in the exponent, r is expressed as $r \equiv r/r_0$, where $r_0 = 1$ μm (i.e. in dimensionless unit equal to micrometer).
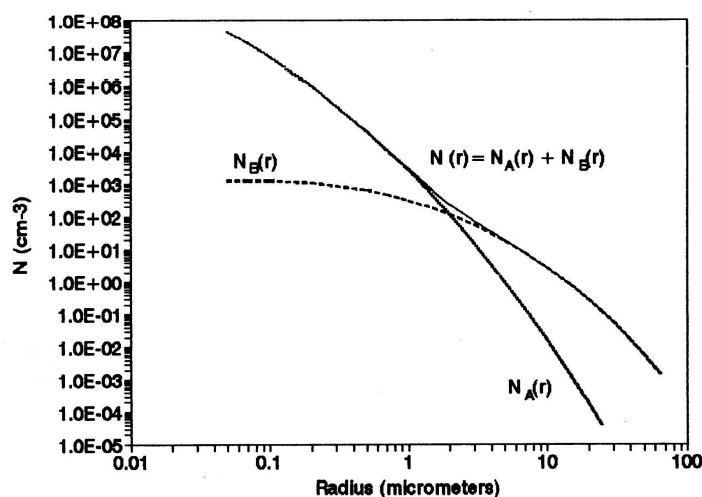

Fig. 2. The two component model of sea particle size distribution (schematic). The A-component is dominant for small sizes, and the B-component for large particle sizes. The slopes of A- and B-component distributions are governed by respective γ-parameter values.

The model (Eqs. 11-13) was developed from analyses of numerous experimental data and represents particle size distribution regardless of mechanisms responsible for its creation. The main difference between the two components is in the general shape (model value, width and skewness) of respective size distribution functions, although one can also argue about some other differences, like predominant composition, particle origin (biogenic or terrigenous), average index of refraction, etc. However, we will show that certain, experimentally determined values of γ-parameters can be related to the coagulation and/or sedimentation mechanisms.

The model is in a very good agreement with experimental results obtained for PSD in various oceans sampled from surface to the depth of 3600 m [15]. Experimentally determined average values for γ_A and γ_B are 0.125 and 0.215 (with standard deviations $\sigma_A = 0.02$, $\sigma_B = 0.01$), respectively.

Although both components span the whole size range, the A-component is dominant at small sizes and the B-component at large sizes of PSD. This is shown in Fig. 2.

Each component-distribution can be piecewise approximated by a power-law. The extent of a sub-range in which this power-law approximation is valid depends (for a given power exponent and the given accuracy of approximation) only on the value of γ-parameter. This is shown in Fig. 3. Sub-range extents ΔR, for which the approximation with power-law $N = Cr^m$ (where m corresponds to a certain mechanism) holds with absolute error in particle number which is less than 10% , versus γ-parameter values are shown in Figs. 4 and 5 for the A- and B-component, respectively. Included range of γ-values corresponds roughly to an interval of 2σ around experimentally determined mean value. Since the A-component is dominant at small particle sizes, and the B-component at large sizes, the exponents assumed in the power-law approximation for the A-component are those corresponding to Brownian, shear coagulation and differential sedimentation, while exponents used for the B-component approximation correspond to shear coagulation and differential sedimentation.
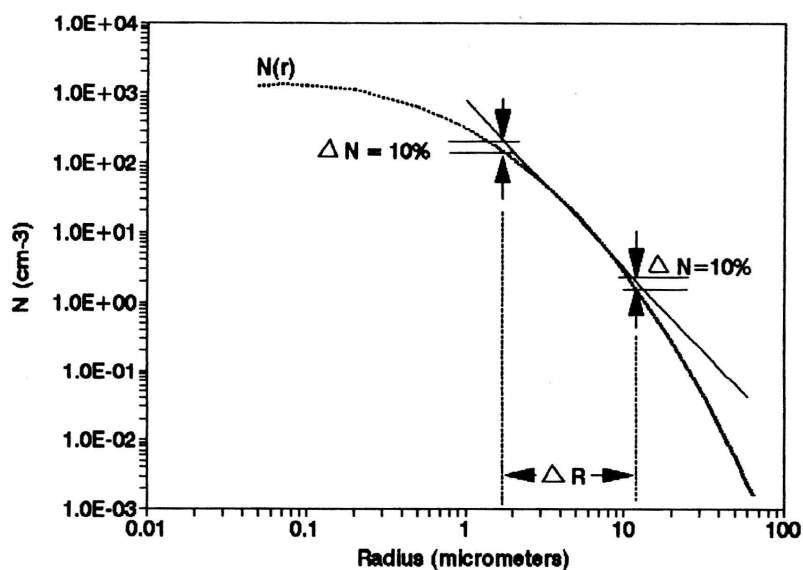

Fig. 3. Aproximation of a particle size distribution by a power-law $N = Cr^m$. The extent of sub-range ΔR in which this approximation is valid depends, for a given m, on acceptable error and skewnes of the distribution.

For the A-component, the size sub-ranges, which can be approximated by power-law with exponents corresponding to Brownian and shear coagulation, are separated for all γ_A-values (Fig. 4). However, while the extent of the sub-range with Brownian coagulation remains nearly constant and limited to a sub-micron particle sizes for all relevant γ_A-values, the extent of the size-range that can be described by the exponent -4 (shear) rapidly shrinks and slowly shifts toward smaller values with increase in γ_A. There is also an overlap with the $m = -4.5$ range, which progressively, with increase in γ_A, "eats" away the $m = -4$ range and becomes adjacent to the Brownian range.

For the B-component there is a substantial overlap between the regions dominated by shear and differential sedimentation for all γ_B-values, and the extent of both size-ranges shrinks (diminishes) with increase of γ_B.
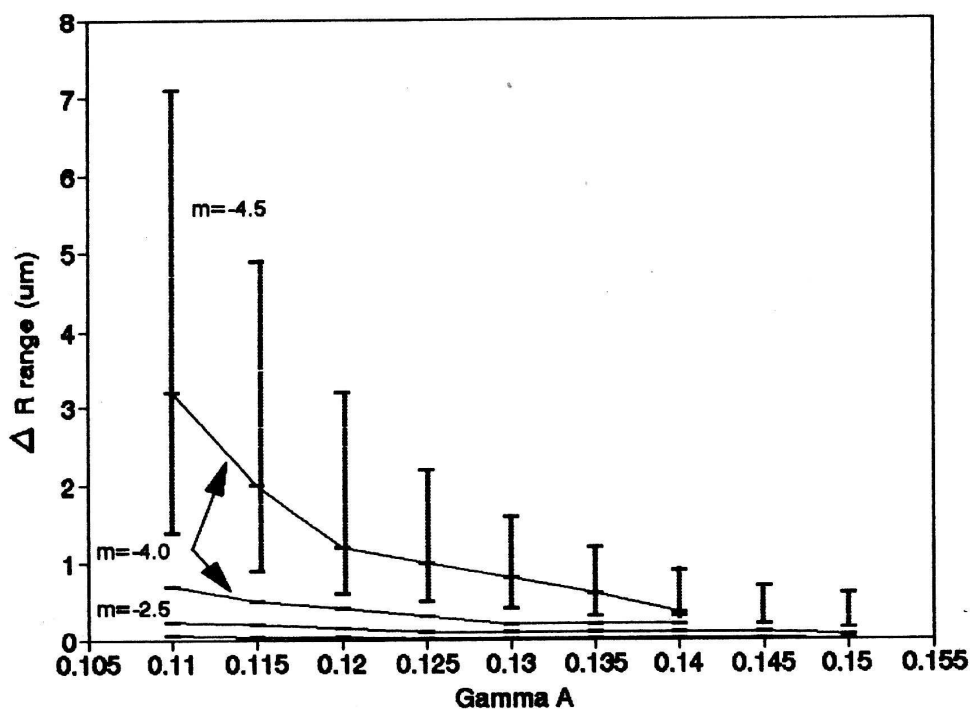

Fig. 4. The A-component particle size sub-range ΔR in which PSD can be approximated with the power-law corresponding to a certain coagulation mechanism, versus γ_A. Shown are the ΔR-sub-ranges for power-law exponents corresponding to Brownian and shear coagulation and differential sedimentation.
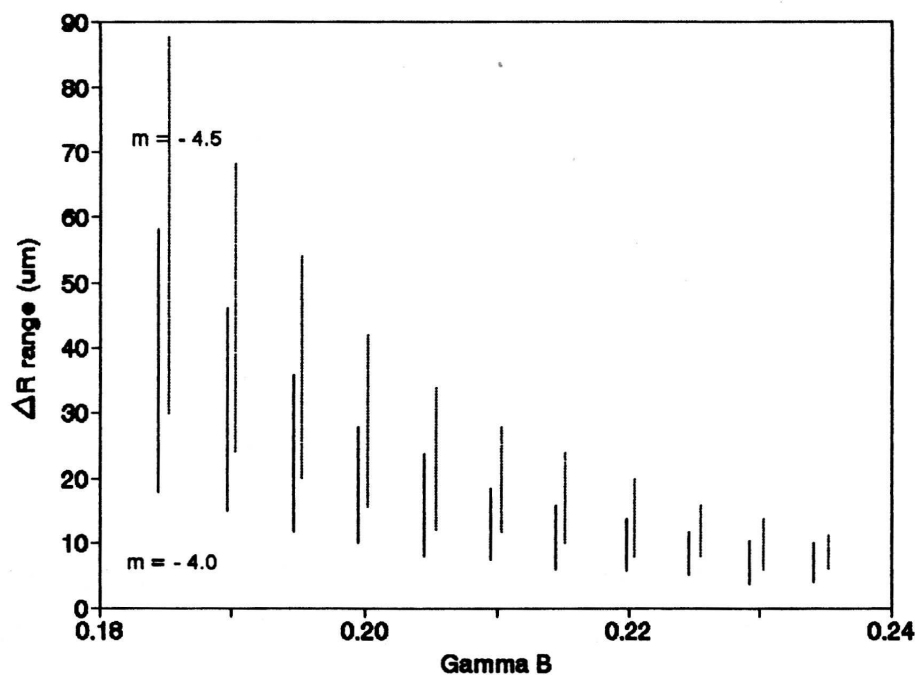
Fig. 5. The B-component particle size sub-range in which PSD can be approximated with power-law corresponding to shear coagulation and differential sedimentation, versus γ_B.

This would indicate that the Brownian motion always dominates the interaction of fine (sub-micron) particles, while differential sedimentation is not limited to a separate (larger) size-range, but rather extends to the smaller sizes or sometimes even dominates over turbulent shear coagulation at small sizes. This result for mechanism/size-range sequence differs from the Brownian-shear-differential sedimentation sequence proposed by Hunt [2], and agrees with recent findings [11]. The difference is due to the assumption that particles, once brought into close proximity (with frequency determined by mechanism-dependent collision function), do indeed make contact. In other words, it was tacitly assumed that contact efficiency is size independent and equal to one. However, recent investigations show that the particle contact efficiency E_{ij} is size dependent and often far below unity. Mc-Cave [4] included the size dependent contact efficiency in calculation of differential sedimentation collision functions, and Hill [11] extended this treatment to shear coagulation. The inclusion of reduced contact efficiency into the calculation dramatically reduced the aggregation rate between particles by turbulent shear, so that even for relatively small particles the contact rates of shear coagulation and

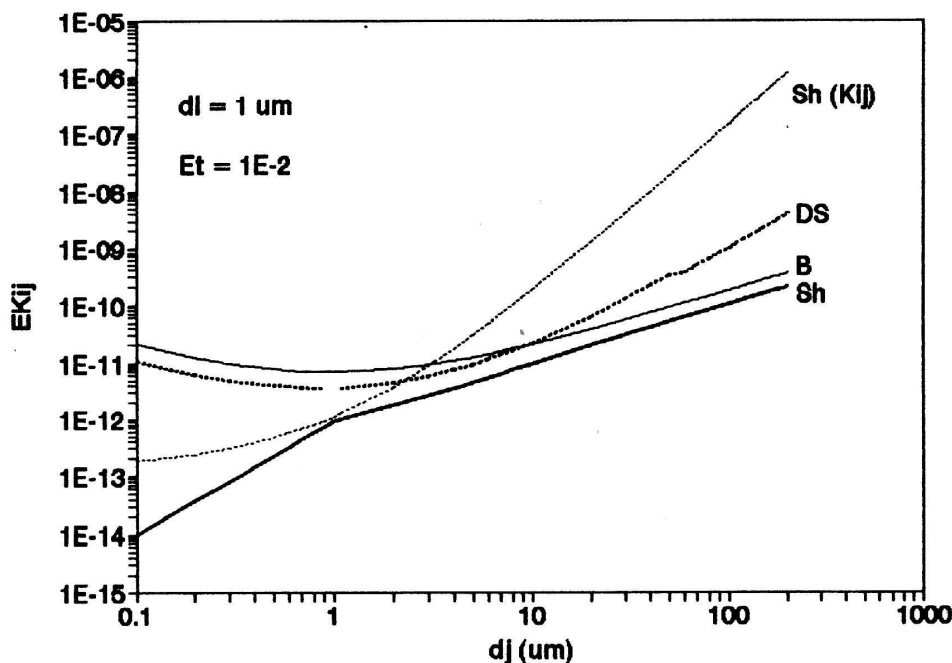differential sedimentation are of similar order. This is shown in Fig. 6.

Fig. 6. Influence of contact efficiency on particle aggregation. Collision function for shear coagulation Sh (K_{ij}) with unit contact efficiency is few orders of magnitude greater than shear collision function Sh (EK_{ij}) calculatet with inclusion of contact efficiency $E \neq 1$. Also shown are the collision functions for Brownian coagulation (B) and differential sedimentation (DS). Turbulent energy dissipation rate E_t corresponds to the surface conditions.

In Figs. 7a−c, we present the products of collision functions for shear coagulation and differential sedimentation given by (4) and (5) with the corresponding contact efficiencies [4,11] for different particle sizes and shear rates. For a high turbulent dissipation rate ($\varepsilon \geq 10^{-2}$ cm^{2}s^{-3}), shear coagulation dominates at small and medium sizes (1-50 μm), while at larger sizes these two mechanisms are of the same order of magnitude. For a lower turbulent dissipation rate, differential sedimentation is dominant over shear coagulation for all sizes. Hence, we may expect that in the deep oceanic waters differential sedimentation dominates in all but very small size-ranges, while at the surface, especially at higher turbulent dissipation rates, shear coagulation would dominate in small and medium size-ranges.
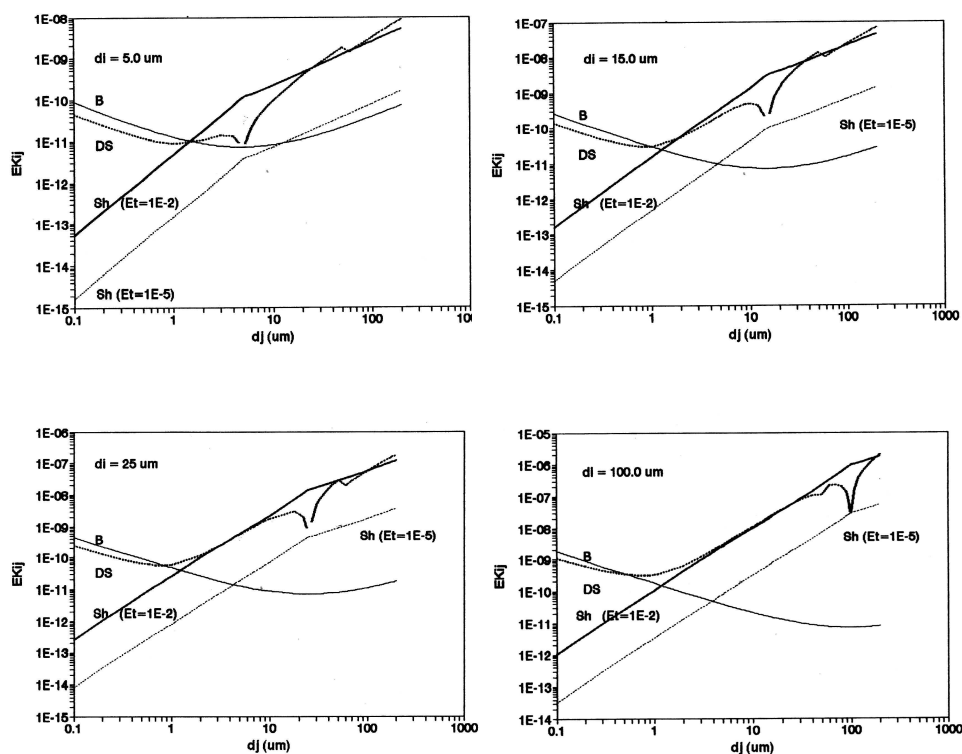
Fig. 7. Collision functions (including contact efficiency $E \neq 1$) for differential sedimentation (DS) and shear coagulation (Sh) for various turbulent kinetic energy dissipation rates. $E_t = 10^{-2}$ $cm^2 s^{-3}$ and $E_t = 10^{-5}$ $cm^2 s^{-3}$ correspond to surface and deep conditions, respectively. Also shown is the collision function for Brownian coagulation (B). a) $d_i = 5$ μm; b) $d_i = 15$ μm; c) $d_i = 25$ μm; d) $d_i = 100$ μm.

Therefore, turning back to Fig. 4, the shrinking of the size extent in which PSD can be approximated by the power-law with exponent -4 (shear), with increase in γ_A, could be interpreted in terms of a decrease in turbulent energy dissipation. Hence, γ_A-values greater than average may be associated with a lower turbulent energy dissipation, a characteristic of deep ocean. To statistically test this hypothesis, we have calculated the average γ_A-values for a set of PSD data from deep ocean [23,27], and for a set of PSD data from the surface and coastal waters [25,26], and then compared these with the average γ_A-value for the TCM model (population mean) inferred from numerous measurements including deep and surface waters [15]. The average value obtained for the deep-water samples ($z > 200$ m) is $\gamma_A^D = 0.158$ ($\sigma = 0.008$) while the average value for the surface is $\gamma_A^S = 0.122$

($\sigma = 0.018$). These differences between the sample means and the population mean are statistically significant at the 95% confidence level. Therefore, we accept the hypothesis and conclude that the high γ_A-values are associated with lower turbulent dissipation rate (characteristic of deep waters) while low γ_A-values are associated with a high turbulent dissipation rate (characteristic of coastal and surface waters).

Hence, small γ_A-values would correspond to a PSD in which shear coagulation dominates at small sizes (sub-micron particles are dominated by Brownian coagulation), followed by overlap region and transition to size-ranges dominated by differential sedimentation and/or settling. The value of γ_B-parameter would determine the width and position of overlap region between shear coagulation and differential sedimentation. The reverse is true for high γ_A-values: a quick transition from Brownian coagulation to differential sedimentation and settling should result in a much faster change of the exponent in the corresponding power-law.

Hence, instead of approximating the PSD piecewise with power-law we may introduce a generalized power-law in which exponent is not constant, but a function of size:

$$\mathrm{d}N(r) = Cr^{m(r)}\mathrm{d}r. \tag{14}$$

The expression for the generalized exponent $m(r)$ can be inferred by equating relation (14) to the TCM (11). One obtains:

$$C_A F_A(r) + C_B F_B(r) = Cr^{m(r)}. \tag{15}$$

Hence:

$$m(r) = \frac{\ln\left[C'_A F_A(r, \gamma_A) + C'_B F_B(r, \gamma_B)\right]}{\ln r} \tag{16}$$

where $C'_A = C_A/C$ and $C'_B = C_B/C$.

For sub-micron sizes ($r \ll 1$) A-component is dominant, so one can neglect the B-component contribution in (15), and solve for C. One obtains:

$$C_A r^2 e^{-52r^{\gamma_A}} = Cr^{m(r)},$$

or

$$\ln C_A + 2\ln r - 52r^{\gamma_A} = \ln C + m(r)\ln r.$$

Regrouping the left-hand side gives

$$\ln C_A - 52 + \left[2 - 52\frac{r^{\gamma_A} - 1}{\ln r}\right]\ln r = \ln C + m(r)\ln r$$

wherefrom

$$\ln C = \ln C_A - 52. \tag{16a}$$

The generalized hyperbolic distribution (14) with $m(r)$ given by (16), although an approximation to the TCM of PSD, when compared to the mechanism-related predictions $(7 - 10)$, lends itself to an easier interpretation.

More or less constant value of $m(r)$ in a given sub-range of particle sizes can be compared with the mechanism-dependent exponents in relations $(7 - 10)$ and interpreted in terms of particular coagulation/sedimentation mechanism. However, relation (16) clearly shows that there are no sharp boundaries between regions with different power-laws (i.e. dominant mechanisms). To the contrary, depending on γ-parameter values there can be a rapid change of $m(r)$ along the size-ranges preventing the association of certain mechanism-related exponent with a given size-range. This in turn indicates that there are two (or even more) mechanisms simultaneously acting in the considered sub-range of which neither one can be neglected.
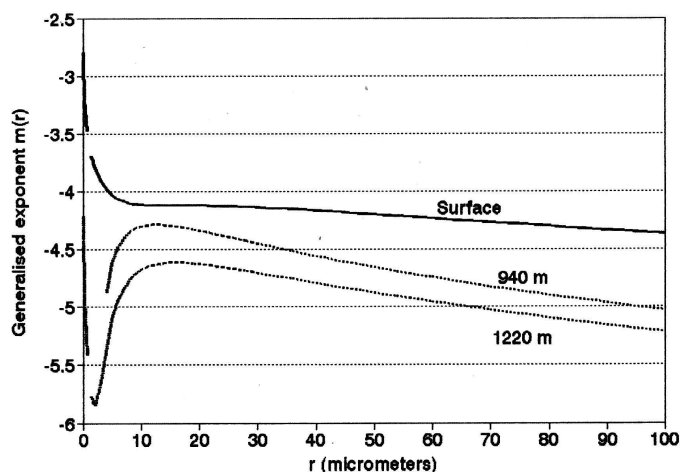

Fig. 8. Generalized exponent $m(r)$ for surface and deep ocean water. Surface value roughly corresponds to shear coagulation for most of the size-range, while deep samples produce $m(r)$ more close to the differential sedimentation and settling.

The generalized exponent $m(r)$ calculated according to (15) for typical samples from the Atlantic [25,26] is shown in Fig. 8. For surface samples, the generalized exponent $m(r)$ is close to -4, and gradually decreases toward -4.5 with increase in particle size. For deep samples $m(r)$ is closer to -4.5 for medium size-range and gradually decreases with size. Both exponents, apart from discontinuity at $r = 1\ \mu$m, increase toward -2.5 for very small sizes ($r \ll 1\ \mu$m). However, $m(r)$ derived for the deep samples, also exhibits an oscillatory behaviour near discontinuity which prohibits decisive conclusions about dominant mechanisms in this region [14]. These values for $m(r)$ are close enough to the values predicted for shear coagulation and differential sedimentation, and are in agreement with expectation. Hence, according to the $m(r)$-behaviour, size/mechanism order for the surface waters is Brownian-

shear-differential sedimentation, with transition regions in between. On the other hand, for the deep waters it seems that differential sedimentation takes the place of the shear coagulation what is in perfect agreement with predictions obtained from considerations of collision functions with size dependent contact efficiency (cf. Figs. 7a-d). Thus, we have shown that the behaviour of generalized exponent $m(r)$ could be associated with the mechanisms underlying PSD.

We must point out that simple theory of PSD, based on few mechanisms described afore, predicts exponent limits of -2.5 and -4.75 for very small and large particles, respectively. However, to successfully represent the measured PSD, a somewhat broader range of exponent must be used. Thus, exponent -1.65 was used for a sub-range of very small particles for distributions measured in the Gulf of Mexico [23], while exponent -5.2 was used for prediction of a very large particle sub-range in digested sewage sludge distribution [24]. The asymptotic values of equivalent $m(r)$, as derived from TCM, agree well with these experimental findings.

4. Conclusions

Dimensional analysis of simple coagulation and sedimentation mechanisms predicts segmented PSD, where size distribution in each segment (size-range) is described by power-law with a characteristic mechanism-dependent exponent. This corresponds to the domination of one coagulation/sedimentation mechanism in a given size sub-range of PSD. Comparison with TCM shows that certain size-ranges in PSD can indeed be described with power-law with characteristic (mechanism related) exponent. However, we found that these size-ranges overlap, indicating that there are two or more concurrent mechanisms simultaneously present in a given sub-range. This overlap is more pronounced in medium and larger size-ranges. On the other hand, we have attributed the rapid shrinking of the size interval associated with shear coagulation with increase of γ_A-value to the change of turbulent kinetic energy dissipation. Comparison of experimentally found γ_A-parameter values for surface and deep ocean PSD data confirmed this hypothesis with high statistic confidence. This is in agreement with the results obtained from comparison of products of contact efficiency with collision function for considered mechanisms. This comparison shows that the differential sedimentation is of the same order of magnitude or greater than shear coagulation for most of the relevant size-ranges, except for the high turbulent dissipation rates associated with surface and coastal waters, where the shear coagulation is dominant for small and medium sizes. For the deep oceanic waters, differential sedimentation dominates over shear coagulation even for small sizes. Very small sizes seem to be always dominated by Brownian coagulation.

The behaviour of respective generalized exponent $m(r)$ is in agreement with these findings and predictions obtained from simple coagulation/sedimentation mechanisms theory of PSD. Therefore, it seems that the behaviour of generalized exponent $m(r)$ inferred from the TCM of sea particle size distribution can be related to the PSD-forming mechanisms.

References

1) J. C. Brun-Cottan, Journal of Geophysical Research **81** (9) (1976) 1601;

2) J. R. Hunt, Advances in Chemistry series, No 189, *Particulates in Water*, M.C. Kavanaugh and J. O. Leckie, Editors, ACS, (1980) 243;

3) I. N. McCave, Deep-Sea Research **22** (1980) 491;

4) I. N. McCave, Deep-Sea Research **31** (1984) 491;

5) D. Lal and A. Lerman, Journal of Geophysical Research **78** (1973) (30) 7100;

6) J. P. Hsu and M. J. Lin, Journal of Colloid and Interface Science **141** (1991) 60;

7) S. S. Honjo, J. Manganini and J. J. Cole, Deep-Sea Research **29** (1982) 609;

8) T. J. Smayda, Oceanography and Marine Biology Annual Review **8** (1970) 353;

9) G. A. Jackson, Deep-Sea Research **37** (1990) 1197;

10) A. L. Alldredge and P. McGillivary, Deep-Sea Research **38** (1991) 431;

11) P. S. Hill, Journal of Geophysical Research - Oceans **97** (1992) 2295;

12) W. Lick, H. Huang and R. Jepsen, Journal of Geophysical Research - Oceans **98** (1993) 10279;

13) T. Kiørboe, K. P. Anderson and H. G. Dam, Marine Biology **107** (1990) 235;

14) D. Risović and M. Martinis, *Prediction of sea particle size distribution from coagulation and sedimentation mechanisms and connection with two-component model*, (1994) to be published;

15) D. Risović, Deep-Sea Research I **40** (7) (1993) 1459;

16) D. Lal and A. Lerman, Journal of Geophysical Research **80** (3) (1975) 423;

17) S. K. Friedlander, Journal of Meteorology **17** (1960) 479;

18) Q. Wang, Journal of Colloid and Interface Science **145** (1991) 595;

19) K. Higashitani, M. Kondo and S. Hatade, Journal of Colloid and Interface Science **142** (1991) 204;

20) P. G. Saffman and J. S. Turner, Journal of Fluid Mechanics **1** (1956) 16;

21) I. E. Torres, W. D. Russel and W. R. Schowalter, Journal of Colloid and Interface Science **142** (1991) 554;

22) S. K. Friedlander, *Smoke, Dust and Haze*, p. 194, John Wiley, New York (1977);

23) J. E. Harris, Deep-Sea Research **24** (1977) 1055;

24) W. K. Faisst, Chapter 12, (258-269) in Advances in Chemistry series, No 189, *Particulates in Water*, M.C. Kavanaugh and J.O. Leckie, Editors, ACS;

25) R. W. Sheldon, A. Parkash and W. H. Sutcliffe Jr., Limnology and Oceanography **17** (1972) 327;

26) R. W. Sheldon (1990), private communication;

27) V. A. Del Grosso, SPIE Vol. **160** (1978) 741.

ULOGA KOAGULACIONIH I SEDIMENTACIONIH MEHANIZAMA U DVOKOMPONENTNOM MODELU RASPODJELE VELIČINE ČESTICA U MORU

DUBRAVKO RISOVIĆ i MLADEN MARTINIS

Institut Rugjer Bošković, P.O.B. 1016, 41001 Zagreb

Razmatraju se jednostavni koagulacioni i sedimentacioni mehanizmi i njihova veza s raspodjelom veličine čestica (RVČ). Pokazano je da se vrijednosti γ-parametra u dvokomponentnom modelu RVČ mogu povezati s koagulacionim i sedimentacionim mehanizmima. Nadalje pokazano je da se male vrijednosti parametra γ_A mogu povezati s visokim iznosima disipacije kinetičke energije turbulencije koji su karakteristični za površinske i priobalne vode. Visoke vrijednosti parametra γ_A, karakteristične za dubinu, induciraju dominaciju koagulacije uslijed diferencijalnog taloženja nad mehanizmom koagulacije izazvane smicanjem. Uvid u raspone veličina u kojima je pojedini mehanizam dominantan, kao i poredak značaja pojedinih mehanizama s promjenom veličine čestica dobiva se iz ponašanja poopćenog eksponenta $m(r)$ hiperbolne distribucije veličina čestica koji je ovisan o parametru γ.